EPJ Web of Conferences **280**, 01002 (2023) https://doi.org/10.1051/epjconf/202328001002
RICAP-22

Ultra-high energy cosmic rays with the Pierre Auger Observatory

Lorenzo Perrone[1,*] for the Pierre Auger Collaboration[2,**]

[1]Universtità del Salento and INFN Lecce (Italy)
[2]Observatorio Pierre Auger, Av. San Martín Norte 304, 5613 Malargüe, Argentina
Full author list: http://www.auger.org/archive/authors_2022_09.html

Abstract.
In the era of multi-messenger astronomy, ultra-high energy cosmic rays offer the unique opportunity to investigate the nature of astrophysical sources and of particle interactions in an energy range far beyond that covered by current particle accelerators. The Pierre Auger Observatory, the world's largest cosmic ray detector, combines in a hybrid design the information from fluorescence telescopes, observing the longitudinal profile of extensive air showers, with a surface array, measuring the lateral distributions of secondary particles at the ground. A review of selected results is presented, focusing on the measurements of energy spectrum and chemical composition and on the search for neutral primary particles. The future prospects will also be discussed in light of the extensive upgrade program being now implemented to further improve the Observatory potential.

1 Introduction

After more than half a century of observations, many of the intriguing mysteries related to the nature and origin of ultra-high energy cosmic rays (UHECRs) remain to be unveiled, though the picture we are reconstructing has now a much higher resolution based on measurements with unprecedented precision. A significant contribution to this field comes from the Pierre Auger Observatory [1] located in the Province of Mendoza, Argentina. The Observatory consists of a surface detector (SD) array of about 3000 km^2 surrounded by 27 air fluorescence detector (FD) telescopes grouped in four sites, providing a powerful instrument for extensive air shower detection. The SD comprises 1600 water-Cherenkov detectors separated by 1500 m (SD-1500) in a triangular grid, plus a smaller nested array of 61 additional detectors spaced by 750 m (SD-750) covering an area of 23.5 km^2. The FD provides a nearly calorimetric estimate of the primary energy, almost independent of the assumptions on hadronic interaction models at the highest energies. The operation of the FD is however restricted to a duty cycle of about 15% because it can operate during moonless nights and it is limited by the atmospheric conditions while the SD measurements are made for about the 100% of the time. The hybrid paradigm relies on the fact that it is possible to calibrate the SD signal using the events simultaneously recorded by the FD, the so-called hybrid events, avoiding to a large extent the use of Monte Carlo simulations and allowing us to achieve good control of the systematic uncertainties in the energy scale [2].

*e-mail: lorenzo.perrone@le.infn.it
**e-mail: spokespersons@auger.org

2 Energy spectrum and composition

The nature and properties of UHECRs and the imprint of propagation effects are embedded in their energy distribution observed at the ground. For this reason, the study of the features characterizing the shape of the energy spectrum has always been among the main goals of the instruments built in this field. The Pierre Auger Observatory can profit from its hybrid design combining a huge accumulated exposure of about 80,000 km^2 sr yr from the SD (SD-1500 + SD-750) with the precise and almost-model-independent energy measurement provided by the FD. The left panel of Fig. 1 shows the energy spectrum for energies above 2.5×10^{18} eV and zenith angles below 60°, derived with more than 200,000 events recorded with the SD-1500 [3]. The SD energy resolution as a function of energy, measured from data, is shown on the right panel in comparison with FD. The systematic uncertainty on the energy scale provided by the FD is 14%, substantially flat in energy and dominated by the calibration of the instrument [2]. The flattening of the spectrum near 5×10^{18} eV (the so-called *ankle*)

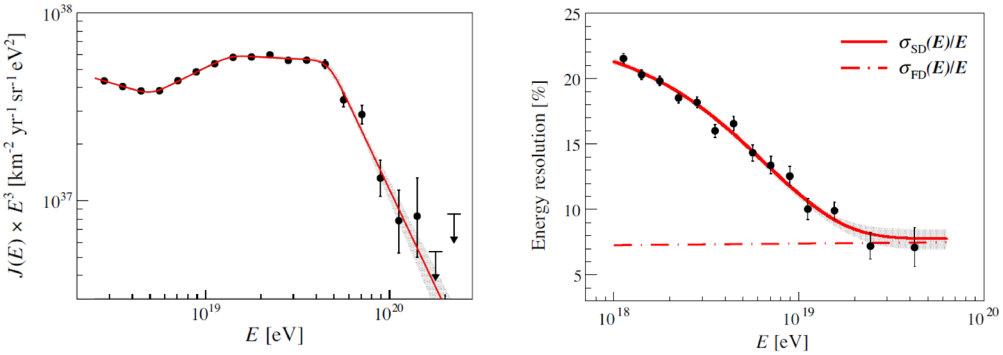

Figure 1. Left: energy spectrum scaled by E^3 and fitted with a broken power-law. The shaded band indicates the statistical uncertainty of the fit. Right: resolution of the SD with statistical uncertainties as a function of energy. The FD resolution is also shown for reference. See [3] for the details about this measurement.

and the subsequent steepening at 5×10^{19} eV are confirmed while a new feature that marks a change from a spectral index of 2.5 to 3.1 named *instep* has been identified in the region above 10^{19} eV. More recently, an extension of the spectrum measurement towards the lower energies has been presented [4] using the SD-750. An inflection of the spectrum starting at about 10^{17} eV is reported, confirming the presence of the so-called *second knee* feature. The combined spectrum SD-1500 + SD-750 is show in Fig. 2, leftmost panel. The energy at which the integral spectrum drops by a factor of two with respect to a power-law extrapolation from lower energies is at about 2×10^{19} eV, which is in tension with that expected for uniformly distributed sources of protons, as also indicated by the results from our composition measurements. Indeed, the average atmospheric depth at shower maximum $\langle X_{\rm max} \rangle$ is directly proportional to the logarithmic mass of the primary particle, while its variance is a convolution of the intrinsic shower-to-shower fluctuations and of the dispersion of masses in the primary beam. The first two moments of the depth of shower maximum as measured at the Pierre Auger Observatory are shown as a function of energy in the central and rightmost panels of Fig. 2. The observed change of growth rate of $\langle X_{\rm max} \rangle$ at $E_{\rm c}$ of about 2×10^{18} eV suggests a non-constant composition that could be interpreted, when comparing with predic-

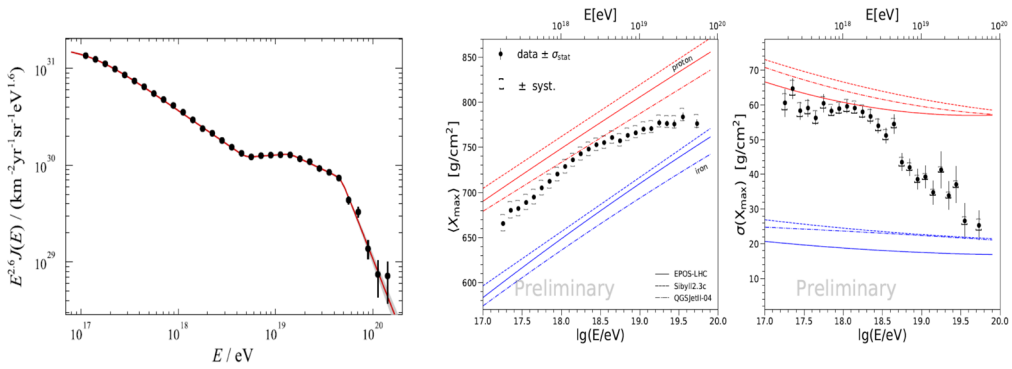

Figure 2. Left: SD energy spectrum after combining the individual measurements by the SD-750 and the SD-1500 scaled by $E^{2.6}$ [4]. Right: the first two moments of the $X_{\max}$ distributions measured by the FD [5].

tions of hadronic models tuned to the most recent LHC results, as an evolution from lighter to heavier elements at the highest energies. The measurement of the standard deviation further supports this result because large values of $\sigma(X_{\max})$ below E_c can be explained as coming from either light or mixed primaries, whereas the subsequent decrease would corresponds to an intermediate to heavy composition.

The measurements of the energy spectrum and mass composition can be combined together with the aim of probing different astrophysical scenarios in terms of source properties, spectral indices at the source, different primary masses and propagation effects [7, 8]. In this context, the flux suppression could be interpreted as mainly due to source exhaustion, rather than to propagation effects. The *instep* would instead reflect the interplay between the flux contributions of the helium and the CNO group injected at the source, shaped by photodisintegration during propagation. In Fig. 3, the contribution of the different mass groups to the energy spectrum and the relative abundances at the top of the atmosphere are shown. The rather large uncertainty on the predicted total fluxes (brown band) is due to combined effects of energy scale and $X_{\max}$ uncertainty. The impact of magnetic fields is not taken into account in these models.

The average composition of UHECRs also appears to be heavier at low than at high Galactic latitudes, the cut being put after a pre-scan at Galactic latitute of 30° [6]. The post-trial significance of this result is currently 4.4 σ. The Galactic magnetic field could be responsible of the mass dependence of the anisotropy, but this effect could be due to the Galactic magnetic field differently affecting different primary masses.

A joint collaboration between the Pierre Auger Observatory and the Telescope Array (TA), a hybrid experiment operating since 2008 in the Northern hemisphere and covering an area of 700 km^2, has started to compare and mutually complement the findings of both experiments. The results on the flux of UHECRs are in agreement within systematic uncertainties up to about 3×10^{19} eV. The difference at higher energies is still under discussion [9]. As for the mass composition, a detailed comparison taking into account the detector effects shows that the TA result is compatible with the mixed composition measured by the Pierre Auger Observatory at least up to 10 EeV [10]. The lack of statistics at the highest energies does not allow TA to distinguish between a mixed, Auger-like composition and a proton one.

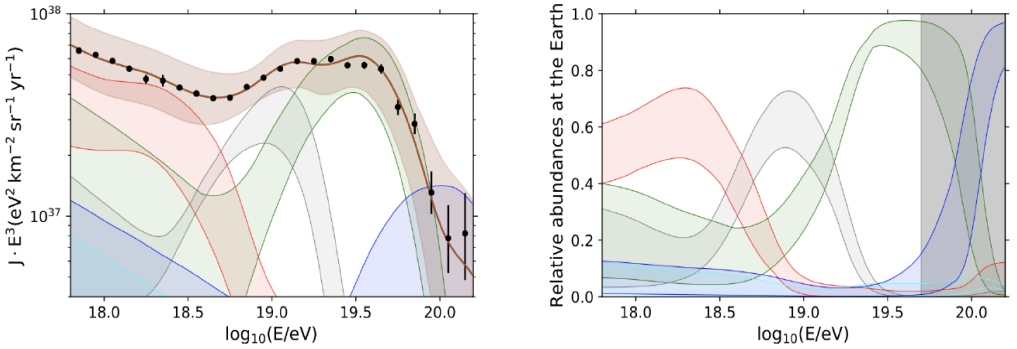

Figure 3. Left: the total energy spectrum (brown) and contribution of various mass group (red: $A = 1$, grey: $2 \leq A \leq 4$, green: $5 \leq A \leq 22$, cyan: $23 \leq A \leq 38$, blue: $A \geq 39$) at Earth predicted by a model [7, 8] fitted to Auger data (black). Right: the relative abundances at the top of atmosphere. The shaded areas indicate the combined effect of systematic uncertainties on E and $X_{\max}$.

3 Anisotropy

The search for anisotropies in the arrival directions of UHECRs is one of the main objectives of the Pierre Auger Observatory's scientific case and a fundamental step towards a coherent interpretation of the observations. This study can be performed at lower energies on large angular scales where the cumulative flux from different sources could possibly be observed despite magnetic deflections. A large-scale dipolar anisotropy in the arrival direction distribution of events recorded by the Pierre Auger Observatory was first observed in [11]. While for energies below 8×10^{18} eV the result is consistent with isotropy, above this energy the first-harmonic modulation in right ascension implies an equatorial dipole amplitude of about 6% with a probability to arise by chance from an isotropic distribution of about 10^{-9}. The sky map in equatorial coordinates is shown in the left panel of Fig. 4. With more than 15 years of data, including events up to 80°, we could exploit the enormous exposure of 120,000 km^2 sr yr. The dipole points $\sim 125°$ away from the Galactic Centre direction, thus suggesting an extra-galactic nature of the UHECRs above this energy. A Galactic origin would result in a much stronger dipole, in a direction within a few tens of degrees of the Galactic Centre.

At energies below 8 EeV, no significant anisotropies were observed, so that relevant upper bounds on the equatorial dipole amplitudes were set down to energies of 0.03 EeV and the right ascension phase of the flux modulations below about 1 EeV is not far from the right ascension of the Galactic Centre. At higher energies, intermediate scale anisotropies can be searched for, as Galactic and extra-galactic deflections of UHECR are expected to be small enough for point sources to be visible as warm/hot spots. The largest available set of events at such energies was obtained thanks to an integrated exposure of 122,000 km^2 sr yr. Some indications of anisotropies at these angular scales, of the order of 25°, have been observed at energies above 41 EeV (right panel of Fig. 4), with the main excess lying around the direction towards the nearby galaxy Centaurus A [12, 13] although other potential sources are located in the same region of the sky, such as the starburst galaxies NGC4945 and M83.

Evidence of a deviation from isotropy has been also found by correlating the arrival directions of UHECRs with the direction of starburst galaxies and active galactic nuclei (AGN) above $\sim 40 \times 10^{18}$ eV, at 4.2 σ and 3.3 σ significance level respectively [12]. This result has been derived accounting for the attenuation of the UHECR nuclei, assuming a mixed mass

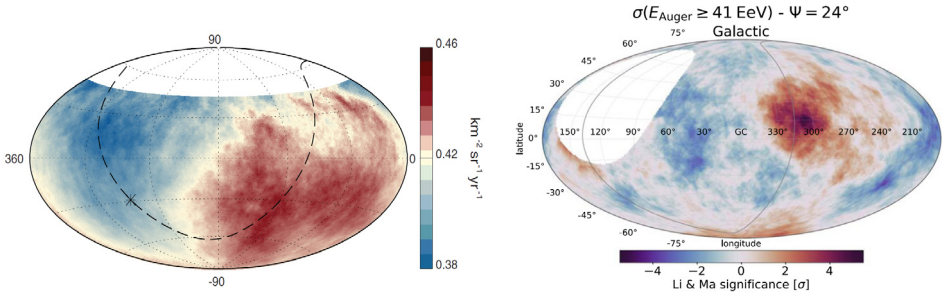

Figure 4. Left: Sky map in equatorial coordinates, using a Hammer projection, showing the cosmic-ray flux above 8 EeV smoothed with a 45° top-hat function. The Galactic Centre is marked with an asterisk; the galactic plane is shown by a dashed line [11]. Right: Local Li–Ma significance map at energies above 41 EeV and within a top-hat search angle of $\Psi = 24°$ in Galactic coordinates [12].

composition as inferred from lower energy observations. The observed correlation does not allow us to disentangle different classes of objects yet; it could furthermore be altered by the effects of Galactic and extra-Galactic magnetic fields.

The comparison with the results obtained by TA allows us to explore possible deviations from isotropy over the full sky. The search for large scale anisotropies over the full sky confirmed the Auger results described above, with reduced systematic uncertainties [14]. Studies on intermediate scale anisotropies found excesses lying along the Supergalactic Plane; about 12% of the events show a correlation with the position of nearby starburst galaxies on a 15° angular scale, with a post-trial significance of 4.2 σ [15].

4 Multi-messengers

UHECRs are mostly protons and other atomic nuclei; a fraction of photons would be an ideal probe for fundamental questions in particle physics and cosmology, such as the nature of dark matter and the possibility of Lorentz invariance violation. Indeed, the decay of super-heavy DM particles could result in large fluxes of UHE Standard Model particles [16], with photons and neutrinos dominating the final state. Also, UHE photons could result from the decay of hadrons produced when protons with $\sim$ 10 the final photon energy interact with microwave/IR/visible/UV background photons, either within the source environment or during their propagation through the intergalactic medium. In the Standard Model, such UHE photons are expected to be quickly absorbed by background photons, but LIV phenomena could inhibit such interactions, resulting in a significantly higher fraction of photons in the UHECR flux. Only UHECR observatories have capabilities to detect photons at these energies, through the extensive air showers they produce in the atmosphere. In this context, the Pierre Auger Observatory has the highest sensitivity to photon primaries. Due to the lower multiplicity of electromagnetic interactions (compared to hadronic), photons induced showers develop deeper in the atmosphere and have less muons thus yielding a larger depth at shower maximum, $X_{\rm max}$, and a steeper lateral distribution function. These distinctive features are also reflected in a longer rise time for the signal shape observed with SD. Since the start of data collection, various searches for ultra-high-energy with energy above 10^{17} eV photons have been performed, either for a diffuse flux, for point sources or for photons associated with transient events such as gravitational wave events. A very recent review of current results in this context can be found here [18] and details about the detection techniques for specific

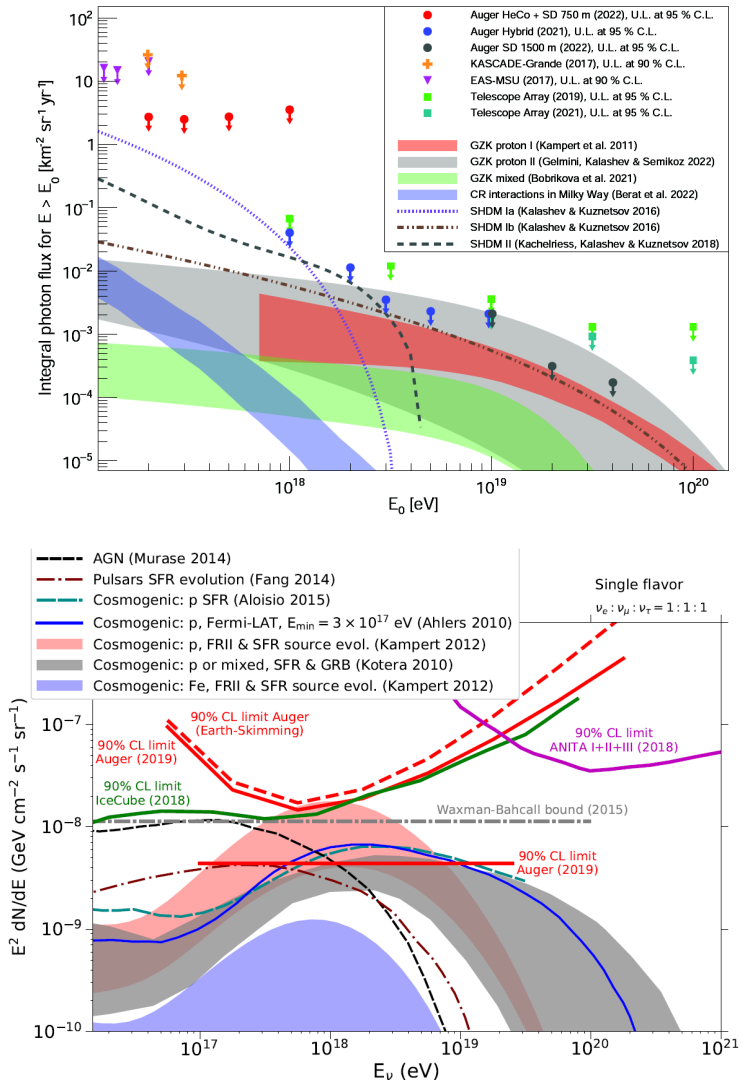

Figure 5. Upper limits on the cosmogenic photons (top) and neutrinos (bottom) fluxes compared to limits from other experiments and to model predictions [19, 20] and references therein.

photon searches have been presented at this conference [17]. As an example, the current status of the search for a diffuse flux of photons is shown in Fig. 5, top panel. Upper limits set by the fluorescence detector operating in hybrid mode play an important role at the lowest and intermediate energies, up the EeV range, those set by the surface detector dominate at the highest energies, above 10^{19} eV.

Several model predictions in the context of dark matter scenarions are severely constrained by the Auger results and also the expectation of photons originating from the interaction of UHECRs with the interstellar medium start to be in tension with a scenario of a proton-dominated chemical composition. Thus, the search of photons can provide strong

bounds on fundamental physics and, at the same time, valuable indications on UHECRs mass composition.

While photons have a limited horizon due to their interaction with the interstellar radiation field (few Mpc at 10^{18} eV), neutrinos can travel substantially unabsorbed over cosmological distances. Their fluxes depend on the properties of the sources and on the composition of the primary beam. Neutrinos can be searched for by selecting horizontal showers with a large electromagnetic component close to the detector. This provides a clear identifier of a neutrino-induced shower as, for hadronic cascades, the electromagnetic component would be almost completely absorbed and only muons could be detected in the SD. Two main categories of events are considered: Earth-skimming, induced by ν_τ travelling upwards from below the Earth crust in directions just below the horizon and producing a τ lepton which can then generate a shower above the SD, and downward-going events due to neutrinos of any flavour. Fig. 5, bottom panel, shows the most recent upper limits on cosmogenic neutrinos [20], along with model predictions and limits from other experiments.

The FD detector is also sensitive to upward-going events and can be used to search for upward-going showers without limitation on the zenith angle of the emerging induced showers. The first results from this study, triggered in the context of what reported by the ANITA Collaboration in the energy range above 10^{17} eV, have been reported here [21].
Given the very good angular resolution of the Observatory (less than 0.5° for zenith > 60°) specific follow-up searches were performed with the SD detector looking for point-like sources in spacial and time coincidence with gravitational waves events: upper limits on the total energy per source radiated in neutrinos [22] and on the photon fluence [23] have been recently set.

5 Dissemination

The Pierre Auger Collaboration is committed to the public release of their data for the purpose of re-use by a wide community including professional scientists, in educational and outreach initiatives, and by citizen scientists. The current policy allows a release of 10% of the cosmic-ray data and 100% of atmospheric data in close-to-raw (JSON) format with summary CSV file containing the reconstructed parameters. In addition to hosting data for downloading, various tools for analysis (with Python notebook examples), event visualisation and a specific outreach section are available on the dedicated website https://opendata.auger.org/. A comprehensive description of this activity is reported here [24].

6 Perspectives

The Pierre Auger Observatory is currently being upgraded within a framework named AugerPrime [25]. The scientific case to be addressed with the upgraded detector includes a better understanding of the origin of flux suppression at the highest energies, the search for a flux contribution of protons up to the highest energies at a level of 10% and the study of extensive air showers and hadronic physics at $\sqrt{s} \sim 70$ TeV. This will require an improvement in the detector ability to identify the composition of primary cosmic rays on an event-by-event basis, which can be achieved in practice by disentangling the muon and electromagnetic components of extensive air showers. The upgrade program includes the deployment of an additional 4m^2 scintillator layer on top of each water-Cherenkov detector [26], an additional small-area photomultiplier tube [27], and an additional radio antenna to observe the radio emission from the electromagnetic component of the shower [28]. The current electronics will also be replaced by faster and newer boards, with sampling frequency of the signals

increased by a factor 3 [29]. Finally, the SD-750 and the SD-433 will be equipped with underground scintillators to provide a direct measurement of the muonic component of the extensive air showers. [30]. All the additional scintillator layers have been installed and about 40% of the array is already equipped with the new electronics. The goal is to complete the deployment by mid-2023. The results of the commissioning data analysis show good uniformity and long-term performance. The Collaboration aims at running the upgraded Observatory until 2030. This would yield an additional vertical exposure of 40,000 km^2 sr yr. Furthermore, a campaign is planned to re-analyze the Phase I dataset by using machine learning techniques, taking at the same time advantage of the AugerPrime Phase II data.

References

[1] The Pierre Auger Collaboration, Nucl. Instrum. Meth. A **798**, 172 (2015).
[2] B. Dawson (Pierre Auger Coll.), PoS(ICRC2019)231.
[3] The Pierre Auger Collaboration, Phys. Rev. D **102** (2020) 062005.
[4] The Pierre Auger Collaboration, Eur. Phys. J. C **81** (2021) 966.
[5] A. Yushkov (Pierre Auger Coll.), PoS(ICRC2019)482.
[6] E. Mayotte (Pierre Auger Coll.), PoS(ICRC2021)321.
[7] E. Guido (Pierre Auger Coll.), PoS(ICRC2021)311.
[8] A. Condorelli (Pierre Auger Coll.), at this conference.
[9] Y. Tsunesada (Pierre Auger and Telescope Array Coll.), PoS(ICRC2021)337.
[10] A. Yushkov (Pierre Auger and Telescope Array Coll.), EPJ Web of Conf. **210** (2018) 010009.
[11] The Pierre Auger Collaboration, Science **357** (2017) 1266-1270.
[12] The Pierre Auger Collaboration,The Astrophysical Journal **935** (2022) 170.
[13] L. Caccianiga (Pierre Auger Coll.) at this Conference.
[14] P. Tinyakov (Pierre Auger and Telescope Array Coll.), PoS(ICRC2021)375.
[15] A. di Matteo (Pierre Auger and Telescope Array Coll.) at this Conference.
[16] R. Aloisio (Pierre auger Coll.), at this Conference.
[17] E. Guido (Pierre Auger Coll.), at this Conference.
[18] The Pierre Auger Collaboration, Universe **8** (2022) 579.
[19] The Pierre Auger Collaboration, Astrop.J. **933** (2022) 125.
[20] The Pierre Auger Collaboration, JCAP **10** (2019) 022.
[21] M. Mastrodicasa (Pierre Auger Coll.), PoS(ICRC2021)1140.
[22] M. Schimp (Pierre Auger Coll.), PoS(ICRC2021)968.
[23] P. Ruehl (Pierre Auger Coll.), PoS(ICRC2021)973.
[24] V. Scherini (Pierre Auger Coll.), PoS(ICRC2021)1386.
[25] The Pierre Auger Collaboration, The AugerPrime Design Report, arXiv:1604.03637.
[26] G. Cataldi (Pierre Auger Coll.), PoS(ICRC2021)251.
[27] A. Castellina (Pierre Auger Coll.), PoS(ICRC2017)397.
[28] F. Schlüter (Pierre Auger Coll.), PoS(ICRC2021)262.
[29] G. Marsella (Pierre Auger Coll.), PoS(ICRC2021)230.
[30] A. M. Botti (Pierre Auger Coll.), PoS(ICRC2021)233.